Supporting Information for:

Permalloy/Polydimethylsiloxane Nanocomposite Inks for Multimaterial Direct Ink Writing of Gigahertz Electromagnetic Structures

Experimental procedure

Ink preparation

The surface modification of permalloy nanoparticles were performed by a silanization reaction as follows. 10 g of permalloy nanoparticles (average size of 70 nm, Shanghai Yaotian nanomaterial CO., Ltd, Shanghai, P.R. China) was added into 50 g of 80 wt.% alcohol aqueous solution and sonicated for 30 mins. 2 g of trimethoxyoctadecylsilane (TMOS, Shanghai Macklin Biochemical Co., Ltd, Shanghai, P.R. China) was added into this solution and vigorous stirred for 8 hours at 60 °C after adjusting pH value to ~ 9. Subsequently, the solution was filtered through a 50 μm screening mesh followed by centrifugation at 3500 rpm for 5 mins. After decanting the supernatant, the precipitate was re-dispersed in 35 mL of ethanol by sonication. The filtering, centrifugation, and re-dispersion processes were repeated for three cycles. After a final precipitation step, the nanoparticles were heated at 80 °C for 8 hours to evaporate the residual solvent and then grinded.

The permalloy/PDMS nanocomposite ink was formulated by adding the appropriate n-hexane (J&K chemical Ltd, Shanghai, R.P. China) into the mixture of base components of PDMS (part A, SE 1700 Clear, DOW chemical Ltd, USA) and the as-prepared TMOS-permalloy nanoparticles. Part B of SE 1700 was then added with a 10:1 base to catalyst weight ratio. The 50 wt.% permalloy/PDMS composite ink was obtained after homogenization at 2000 rpm for 3 mins.

Silver nanoparticles inks were synthesized following a pervious report[1].

3D printing

Multi-material direct ink writing (DIW) was carried out using a custom-made 4-axis micropositioning stage, consisting of two z axis on which two 3cc syringe barrels loaded with the conductive and magnetic inks were connected to two separate fluid dispenser (Performus V, EFD Inc, East Providence, RI, USA). For ink extrusion, Luer-Lock nozzles (160, 210 and 500 μm of diameter, EFD Inc., East Providence, RI, USA) and glass microcapillaries (20 μm of diameter produced using a P-2000 micropipette puller, Sutter Instrument Co., Novato, CA, USA) were attached to the syringe barrels.

All 3D printing processes were performed in ambient conditions with a relative humidity of 20- 40 % and a temperature of 22-27 °C on either glass substrates or silicon wafers.

After printing, the 3D permalloy/PDMS nanocomposite structures were cured at 80 °C for 2 hours. The printed 3D structures with silver features were annealed in 300 °C for 20 mins at a heating rate of 5 °C/min in air in a muffle furnace (KSL-1200X-J, Hefei Kejing Materials Technology Co., Ltd, Hefei, China).

Characterization

Attenuated total reflectance-Fourier transform infrared (ATR-FTIR) spectra were measured using infrared spectrometer (Nicolet iS50, ThermoFisher Scientific Co., Ltd, US) in the range of 4000-400 cm^{-1}. The crystalline structure of permalloy powder and TMOS-permalloy were obtained by powder X-ray diffractometer (D8 Advance, Bruker Co., Ltd, Germany) at scanning rates of 5 degrees per minute in the range between 10 and 80 degrees. The precipitation behaviors of TMOS-permalloy and pristine permalloy nanoparticles in suspension were evaluated by mixing 1 wt% nanoparticles with n-hexane under 30 min sonication and then stewing at room temperature for a certain time. The hysteresis(B-H) loops were measured using a physical property measurements system (PPMS Dyna-cool 9, Quantum Design Co., Ltd, US) and the permeability was measured using vector network analyzer (PNA-N5245A, Agilent Technologies Co., Ltd, US) in the frequency range of 0.1-11 GHz. All magnetic properties were performed in ambient condition. TG-DTG curves were obtained using thermal analysis (TGA/DSC 3+/1600 HT, Mettler-Toledo Co., Ltd, Switzerland) at heating rates of 10 °C/min in air. The rheological properties of the inks were investigated with a controlled stress rheometer (Discovery HR 10, TA Instrument Co., Ltd, US), using a 25 mm-diameter plane plate with 500 μm gap between the parallel plates at 25 °C. Ink viscosities were measured as a function of shear rate from 0.1 to 100 s^{-1}. Storage and loss moduli were measured as a function of stress amplitude range of 50 to 4000 Pa at a frequency of 1 Hz. The morphology of various printed structures was examined by scanning electron microscope (Gemini450, Carl Zeiss Co., Ltd, Germany). Element distribution was performed by energy dispersive X-ray spectrometry detectors (Extreme, Oxford instrument, UK).

The electromagnetic properties of 3D printed passive devices were characterized in the frequency range of 0.1 GHz to 12 GHz by microwave scattering analysis using an

Agilent vector network analyzer (PNA- N5247A, Agilent Technologies Co., Ltd, US). Measurements were carried out on a probe station equipped with two ground-signal-ground (GSG) microwave probes (Summit 11000B-M, Cascade Microtech Co., Ltd, US). 1-port scattering analysis was used for inductors and capacitors and 2-port scattering analysis was used for LC resonators. The measured 1-port and 2-port S parameters of electromagnetic devices were converted to Y parameters for the performance of inductor and capacitor and the impedance of LC resonator. Specifically, the inductance, capacitance and the corresponding quality factor were extracted from the measured Y parameters versus frequency according to the following formulae:

$$L = \frac{\mathrm{Im}(\frac{1}{Y})}{2\pi f} \quad (1)$$

$$Q_L = \frac{\mathrm{Im}(\frac{1}{Y})}{\mathrm{Re}(\frac{1}{Y})} \quad (2)$$

$$C = \frac{\mathrm{Im}(Y)}{2\pi f} \quad (3)$$

$$Q_c = \frac{\mathrm{Im}(Y)}{\mathrm{Re}(Y)} \quad (4)$$

Where L, Q_L, C, Q_c and f are respectively the inductance, the quality factor of the inductor, capacitance, the quality factor of the capacitor and frequency.

Table S1. Wavenumbers and corresponding types of vibration in the FTIR spectra.

Wavenumber (cm^{-1})	Type of vibration	Reference
3440	H-O-H stretching	[2]
2916	CH2 antisymmetric stretching	[3]
2848	CH_2 symmetric stretching	[3]
1627	H-O-H stretching	[2]
1469	C-H scissoring	[3]
1088	Si-O stretching	[4, 5]
954	Fe-O-Si stretching	[4, 5]
780	Si-O-Si symmetric stretching	[4, 5]
581	Fe-O stretching	[4, 5]
563	Fe-O-Si	[4, 5]
468	Si-O-Si or O-Si-O bending	[4, 5]

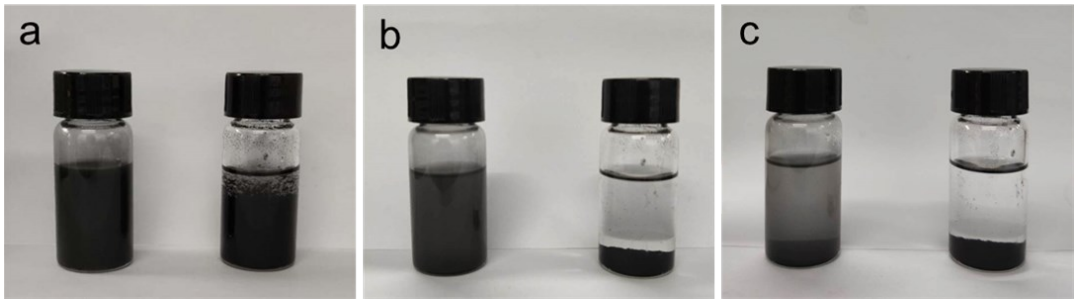

Fig S1. Sedimentation of the TMOS-permalloy (left) and pristine permalloy (right) nanoparticles in n-hexane: (a) after 1 minute, (b) after 2 hours, (c) after 12 hours.

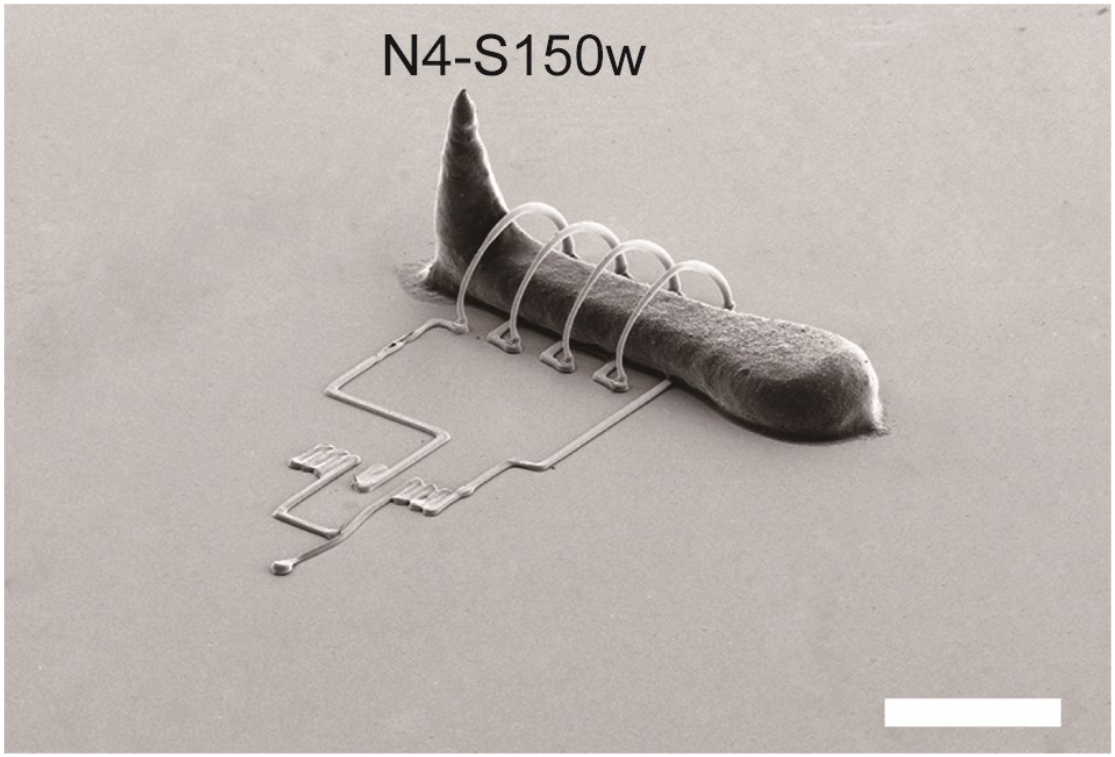

Fig. S2. SEM image of the printed inductor integrated with a magnetic core (N4-S150w sample, scale bar: 400 μm).

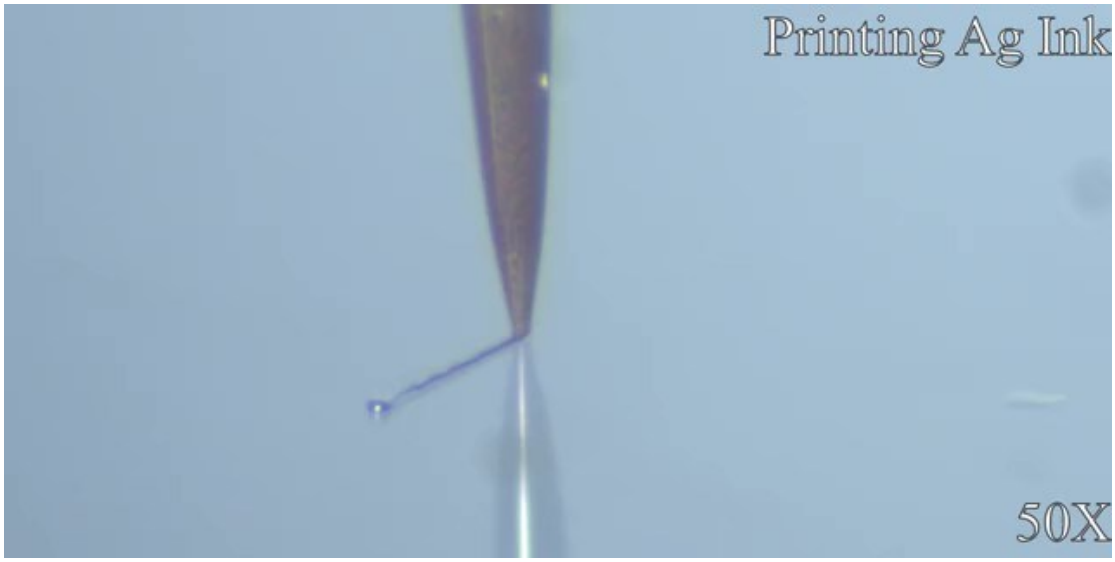

Movie S1. Multimaterial Direct ink writing of silver nanoparticle ink and permalloy/PDMS ink through a 20 μm and a 160 μm nozzle, respectively, to create a magnetic-core solenoidal inductor. The video was captured using a high-resolution camera mounted on both Z-axis of the micropositioning stage.

Table S2. Comparisons of the material compositions and performance of the inductors and the corresponding fabrication methods in published reports.

Inductance (nH) @1GHz	self-resonate frequency (GHz)	Coiling materials	Core materials	Major method	Reference
10	6	Ag	Permalloy/PDMS	3D printing	This paper
5	13	Ag	_____		6
0	0.23	Ag	UV curable polymer		7
2	18.6	Ag	_____		8
0	0.8	silver-organo-complex	Fe_3O_4	Inkjet printing	9
8	4	silver-organo-complex	Ultraviolet-cured polymer		10
8	6.5	Ag	SU-8 polymer		11
8.3	7	Si/Al	_____	MEMS	12
0.38	>10	Cr/Cu	_____		13
6	15	Cu	_____		14
4	10	Cu	_____		15
14	3.8	multimetal	_____		16
1.2	>10	Cr/Au	Su-8 polymer		17
1.93	6	Cu	Permalloy/SiO_2		18
4.4	14.5	Cu	Ni/Al_2O_3		19
3	2	-	NiFe/Cr		20
0	0.3	Cu	CoZrTa		21

References:

1. B. Y. Ahn, E. B. Duoss, M. J. Motala, X. Guo, S. I. Park, Y. Xiong, J. Yoon, R. G. Nuzzo, J. A. Rogers and J. A. Lewis, Science, 2009, 323, 1590-1593.
2. Z. Xu, J. Yu, G. Liu, B. Cheng, P. Zhou and X. Li Dalton Trans., 2013, 42, 10190-10197.
3. M. P. Quiroga Argañaraz , J. M. Ramallo-López , G. Benítez , A. Rubert , E. D. Prieto , L. M. Gassa , R. C. Salvarezza and M. E. Vela, Phys. Chem. Chem. Phys.,

2015, 17, 14201-14207.
4. J. O. Park, K. Y. Rhee and S. J. Park, Appl. Surf. Sci., 2010, 256, 6945-6950.
5. B. Zhou, Z. Liu, X. Wang, Y. Sui, X. Huang, Z. Lu and W. Su, Physica B, 2010, 405, 374-378.
6. N. Zhou, C. Liu, J. A. Lewis and D. Ham, Adv. Mater., 2017, e1605198.
7. Y. Gu, D. Park, D. Bowen, S. Das and D. R. Hines, Adv. Mater. Technol., 2018, e1800312.
8. A. B. Menicanin, L. D. Zivanov, M. S. Damnjanovic and A. M. Maric, IEEE Transactions on Electron Devices, 2013, 60, 827-832.
9. M. Vaseem, F. A. Ghaffar, M. F. Farooqui and A. Shamim, Adv. Mater. Tech., 2018, 3, e1700242.
10. G. McKerricher, M. Vaseem and A. Shamim, Microsyst. Nanoeng., 2017, 3, e16075.
11. B. S. Cooket, C. Mariotti, J. R. Cooper, D. Revier, B.K. Tehrani, L. Aluigi, L. Roselli and M. M. Tentzeris, 2014 IEEE MTT-S International Microwave Symposium (IMS2014), Tampa, 2014, 1-4.
12. S. Chang and S. Sivoththaman, IEEE Electron Device Letters, 2006, 27, 905-907.
13. D. Fang, Q. Yuan and X. Li, Microsyst Technol., 2010, 16, 2119-2122.
14. X. Han, W. Wu, Z. Li, Y. Hao and G. Yan, Thin Solid Film, 2006, 515, 2607-2611.
15. X. Wang, X. Zhao, Y. Zhou, X. Dai, and B. Cai, IEEE Transaction on Electron Devices, 2004, 51, 814-816.
16. M. C. Hsu, T. Y. Chao, Y. T. Cheng, C. M. Liu, C. Chen, IEEE Transactions on Nanotechnology, 2009, 8, 281-285.
17. Yong-Kyu Yoon, Jin-Woo Park and M. G. Allen, J. Microelectromech. Syst., 2005, 14, 886-894.
18. J. zhao, J. Zhu, Z. Chen and Z. Liu, IEEE Transactions on Magnetics, 2005, 41, 2334-2338.
19. M. C. Hsu, T. Y. Chao, Y. T. Cheng, C. M. Liu, C. Chen, IEEE Transactions on Nanotechnology, 2009, 8, 281-285.
20. T. Dastagir, W. Xu, S. Sinha, H. Wu, Y. Cao and H. Yu, Appl. Phys. Lett., 2010, 97, 162506.
21. D. S. Gardner, G. Schrom, F. Paillet, B. Jamieson, T. Karnik and S. Borkar, IEEE Trans. Magn., 2009, 45, 4760-4766.